OPEN

Single molecular investigation of DNA looping and aggregation by restriction endonuclease BspMI

Yanwei Wang, Shiyong Ran & Guangcan Yang

School of Physics and Electronic Information, Wenzhou University, Wenzhou 325035, China.

DNA looping and aggregation induced by restriction endonuclease BspMI are studied by atomic force microscopy (AFM) and magnetic tweezers (MT). With Ca^{2+} substituted for the normal enzyme cofactor Mg^{2+} and enzyme concentration below the critical concentration of 6 units/mL, AFM images of DNA-BspMI complex show that the number of binding and looping events increases with enzyme concentration. At the critical concentration 6 of units/mL, all the BspMI binding sites are saturated. It is worth noting that nonspecific BspMI binding to DNA at saturation concentration represents more than 8% of the total BspMI-DNA complexes directly observed in AFM images. Furthermore, we used MT to prove that additional loops can form when enzyme concentration is higher than its saturation valueand the complex is incubated for a long time (>2 hrs). We ascribe this phenomenon to the aggregation of enzymes. The force spectroscopy of the BspMI-DNA complex shows that the pulling force required to open the loop of the complex at less than saturation concentration has a peak at about 3 pN, which is lower than the force required to open additional loops due to enzyme aggregation at higher than saturation concentration (>6 pN).

Site-specific protein-DNA interactions play a fundamental role in many biological processes like DNA repair, DNA replication and DNA transcription[1,2]. Many methods, such as magnetic tweezers (MT)[3], optical tweezers (OT)[4], electron microscopy (EM)[5–8] and atomic force microscopy (AFM)[9–17], have been used for investigating specific protein-DNA complexes at single-molecule level.

A host of fundamental biochemical processes rely on protein interactions with multiple DNA sites via DNA looping. DNA looping interactions can enhance or repress gene expression. Two-site restriction endonucleases (REases) acting on long linear DNA molecules provide a model system for studying protein-mediated DNA looping[18]. A number of proteins can sense the relative orientations of two sequences at distant locations in DNA: some only bind to sites in inverted (head-to-head) orientation, while others require sites in repeat (head-to-tail) orientation. The Type IIS enzyme BspMI recognizes the asymmetric sequence 5′-ACCTGC-3′ and cleaves top and bottom strands 4 and 8 bases downstream of this site, respectively. Its target is an asymmetric sequence, so two sites in repeat orientation differ from sites in inverted orientation[19]. The profile of the steady-state reaction of BspMI on its two-site substrate is thus similar to those of the tetrameric type IIf restriction endonucleases, such as SfiI, Cfr10I, and NgoMIV[7,19–22]. Further studies described by Halford et al. show that BspMI exists in solution as a tetramer of identical subunits, which has to bind to two copies of its recognition sequence before cleaving DNA[23]. It converts DNA with two sites directly to the final products cut at both sites without liberating intermediates cut at one site[24].

DNA loops induced by some enzymes have been directly imaged by EM[5–8]. EM studies demonstrate that two distant recognition sites are brought together through DNA looping. The Griffith group used EM to demonstrate that NaeI endonuclease simultaneously binds to multiple recognition sites in pBR322 DNA to form loops. The maximum number of loops formed with a common base suggests four binding sites per enzyme molecule[6]. Pingoud et al. suggest that the dimeric form of Sau3AI supplies two DNA-binding sites: one that is associated with the catalytic center and another that serves as an effective site[8]. In addition to the EM studies, there have been numerous AFM investigations involving protein-DNA constructs[10,25,26]. Visualization of specific DNA loops in the protein-DNA constructs was achieved by improved sample preparation and analysis techniques[10]. A Type I DNA-binding restriction enzyme EcoKI monomer binds to DNA at a random sequence to form a dimer, indicating that dimerization does not occur before DNA binding. The other result is that dimerization takes place on specific sites before any looping or before the two specific sites are bound together. There are many
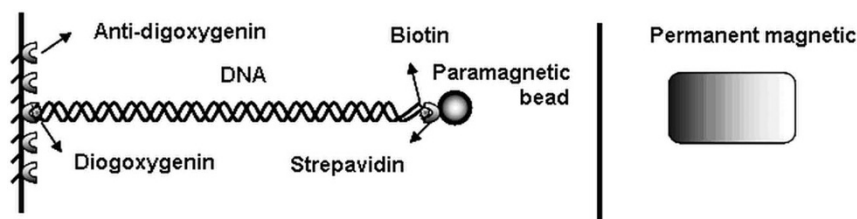
Figure 1 | Bead-DNA-sidewall constructs for single-molecule MT experiment. The polished surface of the flow chamber was treated with polydimethylsiloxane and anti-digoxygenin in order to link the digoxygenin-end of λ-DNA. DNA-bead construct was then flowed into the cell to form a side wall-DNA-paramagnetic bead structure.

protocols for studies of structure and dynamics of DNA and protein-DNA complexes with atomic force microscopy (AFM)[25,26]. Looping in linear lambda DNA induced by enzyme BspMI has been studied by using MT with loop sizes ranging from about 90 to 1500 bp[3]. This experiment indicated that the looping of DNA by BspMI can be controlled using force, and that the critical force needed to open the loops under specific solution conditions is 1.75 ± 0.25 pN. Additionally, Smith et al.[4] used single DNA optical tweezers manipulation to study eleven cases of sixteen known or suspected two-site endonucleases (BpmI, BsgI, BspMI, Cfr10I, Eco57I, EcoRII, FokI, HpaII, NarI, Sau3AI and SgrAI). They found that DNA looping is highly variable depending on not only the mechanical properties of DNA, but also the characters of the specific protein involved.

In this paper, we measured the DNA looping and aggregation induced by restriction of endonucleases BspMI using AFM and MT. The saturation concentration of DNA binding sites is 6 units/mL. At concentrations below this value, the number of binding events to one site and binding to two sites of looped DNA increased with concentration. At saturation concentration, there are more than 39 sites to bind enzyme to a single DNA molecule. Nonspecific binding constituted on average 8% of all binding events. Thus, the normal loops induced by binding of two sites do not form easily at the saturating concentration. The additional loops induced by enzyme aggregation formed when the enzyme concentration was higher than the saturation concentration and when the incubation time was longer. Using MT, we quantitatively analyzed the force required to disrupt two kinds loops. The force needed to disrupt normal loops with two binding sites was lower than that for other kinds of loops formed with enzyme aggregates.

Methods

DNA and enzyme. Bacteria λ-phage DNA was purchased from New England Biolabs and used without further purification. As received from the manufacturer, the λ-phage DNA stock solution had a concentration of 500 ng/μL. The solvent was 1 × TE buffer, which was composed of 10 mM Tris-HCl, pH 8.0, and 1 mM EDTA. Restriction enzyme BspMI was purchased from New England Biolabs too, with a concentration of 5 units/μL. Water was deionized and purified by a Millipore system and had a conductivity less than $1 \times 10^{-6} \, \Omega^{-1} cm^{-1}$. Mica was cut into approximately 1 cm² square pieces and mica surfaces were always freshly cleaved before use. Other chemicals were all purchased from Sigma-Aldrich. The experiments for MT were conducted in phosphate-buffered saline (PBS) (PH = 7.5, 140 mM NaCl). The binding buffer in MT was PBS with 100 μM of added CaCl₂.

AFM imaging. Imaging was performed in Tapping Mode with a Multimode AFM (SPM-9600, Shimadzu, Kyoto, Japan). All samples were imaged in air using tapping mode with root mean square amplitude of about 2 V and drive frequency of about 320 kHz. Commercially available silicon probes with a specified spring constant of 42 N/m were employed. The length, height, and width of the DNA and protein in AFM imaging were measured manually using the off-line analysis software with AFM.

AFM sample preparation. The stock solution of 500 ng/μL λ-DNA was diluted with binding buffer containing 10 mM Tris-HCl, 50 mM NaCl, and 10 mM CaCl₂. The final concentration of DNA was thus 1.25 ng/μL. Experiments were performed by mixing different amounts of BspMI to DNA solution. Samples were incubated at 37°C for 30 minutes and sometimes for more than 2 hours. A 15 μL liquid of the mixture was deposited onto freshly cleaved mica for 2 minutes. Then the mica surface was rinsed 10 times with 200 μL Milli-Q filtered water to remove excess molecules and subsequently dried using a gentle stream of nitrogen gas.

Data analysis of afm. Data regarding the binding ratio and the rate of DNA loop formation were obtained from at least twenty different mica samples. About 50 DNA molecules were analyzed for each mica sample from different 5 × 5 μm² areas. The mean values of the ratio of DNA binding to the number of DNA loops were then plotted for the twenty samples. The variance between the twenty samples did not exceed 20%. The reported rates of binding and loop formation have been normalized using the maximum value.

We plotted the volume distribution of the protein in our AFM experiment. The molecule volume of the protein particles was determined from particle dimensions derived from AFM images. This was calculated using an adjusted version of the equation used in the previous AFM investigations on EcoKI[9]. The height (h) and basal radius (r) of each protein molecule were measured and used to calculate the molecular volume withthe expression

$$V_m = (\pi h/6)(3r^2 + h^2) \qquad (1)$$

Eq. 1, which treats the particle as a spherical cap[27]. For individual protein complexes associated with DNA, heights and radii were measured independently using the SPM-9600 software.

Magnetic tweezers setup. We used magnetic tweezers similar to the one recently developed by Sun et al[28]. The flow chamber was described in detail in the reference and the polished surface was treated with polydimethylsiloxane and anti-digoxygenin in order to link the digoxygenin-end of λ-DNA. DNA-bead construct was then flowed into the cell to form a side wall-DNA-paramagnetic bead structure in PBS buffer[29,30] (Figure 1). The distance between the bead and the surface of the sidewall can be deemed as the extension of DNA. The applied force was calculated according to Brownian motion of the microsphere in the direction perpendicular to the DNA extension. The analysis of the extension was determined by a tracking algorithm of fast Fourier transform-based correlation techniques[29]. After checking a single suspending λ-DNA, diluted protein solution in PBS buffer with 100 μM of added CaCl₂ was loaded to the chamber and the elastic response of DNA as a function a time was recorded and analyzed at different forces.

Single-molecule measurements. We injected the microsphere-bound DNA molecules into the flow cell, and put the cell perpendicularly for 30 min at room temperature, making for the polished edge surface of the cover glass below. After the DNA ligated the polished edge, we rinsed the cell with buffer to clean out the free particles. We then found a ligated particle and confirmed that it was connected to the surface through a single DNA molecule. Then different concentrations of BspMI were injected to the flow cell, in which the force is large enough to pull the DNA that the couture length is about 95%. Afterwards, we took off the magnetic force so that the DNA molecule could exist with full flexibility for about 30% of the couture length. After incubation for different times, we then increased force to determine at what force the DNA loop would open. DNA extension was recorded in real-time.

Results and discussion

Specific and nonspecific binding of BspMI on lambda DNA. In the presence of Mg^{2+}, BspMI recognizes the asymmetric sequence and cleaves top and bottom strands 4 and 8 bases downstream of this site, respectively. By replacing Mg^{2+} with Ca^{2+}, the BspMI cannot cleave the DNA, and forms the BspMI-DNA loops by two sequences[24,31]. In the λ-DNA molecule the binding sequence occurs 41 times. However, the two sites near base pair 39,681 are separated by 3 bp and those near base pair 37,003 overlap. Thus, the number of available binding sites is only 39 with the possibility of forming up to 19 different loops. AFM was used to visualize the BspMI-DNA complex on Ca2+ coated mica at a concentration of 6 units/mL. At this concentration, all the DNA binding sites are saturated. Occasionally the images revealed pure protein in the absence of DNA on mica surface. Occurrence of pure BspMI on mica was nevertheless rare, since BspMI does not bind to mica (Figure 2).
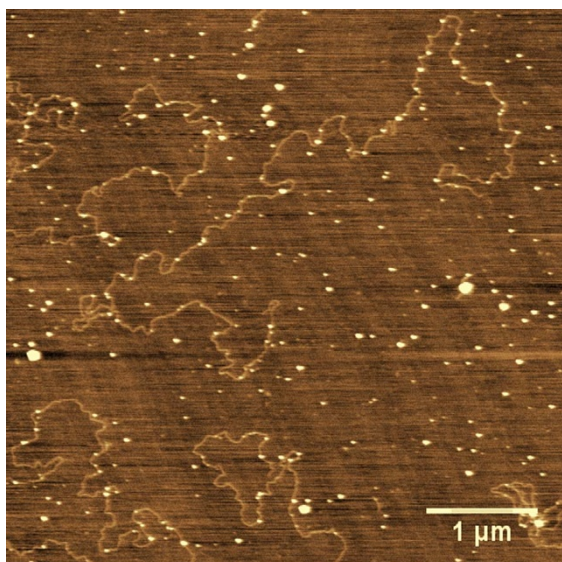
Figure 2 | AFM images of BspMI-DNA complex at the saturation concentration of 6 units/mL. AFM images showed more than 39 bound protein particles attached along the lambda-DNA at the saturation enzyme concentration. Non-specific binding sites constituted over 8% of all binding events. Loops are hard to form when the binding sites are occupied by bound enzymes.

The enzymes of BspMI are tetramers in solutions. The dimensions of BspMI can be measured by AFM. The absolute x-, y-, and z-dimensions of the particles are distorted due to the size and shape of the individual tip used to image them. Within a scan or set of scans using the same deposition and the same tip, the dimensions of different DNA molecules and their corresponding x-, y-, and z-distortions have been shown to remain constant[32]. Accordingly, we have not attempted to correct for the distortions of absolute size. We compared relative sizes of protein complexes within one scan set, pure protein in the absence of DNA, as well as protein bound to the DNA. Measurements showed that the unbound protein height was

2.0 ± 0.2 nm and the diameter at half height was 23.0 ± 1.5 nm (n = 25). Modelling molecules as spherical segments and using these dimensions, we determined the volume of a single protein molecule to be 423 ± 4 nm³. Along these lines, the volumes of all particles in a sample were calculated based on their dimensions. For further analysis we only selected particles whose calculated volumes were about 420 nm³, corresponding to single unbound protein molecules. Note that the statistics for particle diameter and height is valid only for this specific ensemble and the corresponding volume is only used for relative comparison. Furthermore, when interpreting scanning data, one has to consider that the sample signal is convolved with that of the AFM tip. For example, the measured width of DNA by AFM is usually about 10 to 20 nm while its real width is 2 nm. The real diameter of the particle of particles can be obtained by the expression $r \approx \frac{D^2}{16R}$ [33], where D is the diameter based on direct measurement from the AFM image and R is the tip radius of curvature. The tips we employed for imaging (Nanoworld NCHR-20), had a radius of curvature of about 8 nm, as specified by the manufacturer. Thus, real particle diameter was determined to be r ≈ 4.13 nm and the corresponding volume about 295 nm³, which is well within the range of typical proteins.

In Figure 2, we measured the volume of the enzyme molecules bound to DNA. These molecules had a diameter at half-height of 22.0 ± 3 nm and a height of 2.0 ± 0.1 nm (n = 30), giving an estimated single molecule volume of 384 ± 27 nm³. This change in volume between free enzyme molecules and DNA bound molecules is significant. It might be related to its tight binding to DNA and the adsorption of the resulting complex to mica surface. This phenomenon has been observed elsewhere for EcoKI as well[9].

AFM images showed more than 39 bound protein particles attached along the lambda-DNA at saturated enzyme concentrations. The volumes of these protein particles suggest that each site was bound to one tetramer-DNA complex. Such saturation of binding sites inhibits loop formation by BspMI because each BspMI needs to bind to exactly two binding sites in order to form a loop. In the λ-DNA molecule this binding sequence exists 39 times. We observed that nonspecific binding comprised over 8% of all bound proteins, as shown in Figure 2. We occasionally observed that the loop would
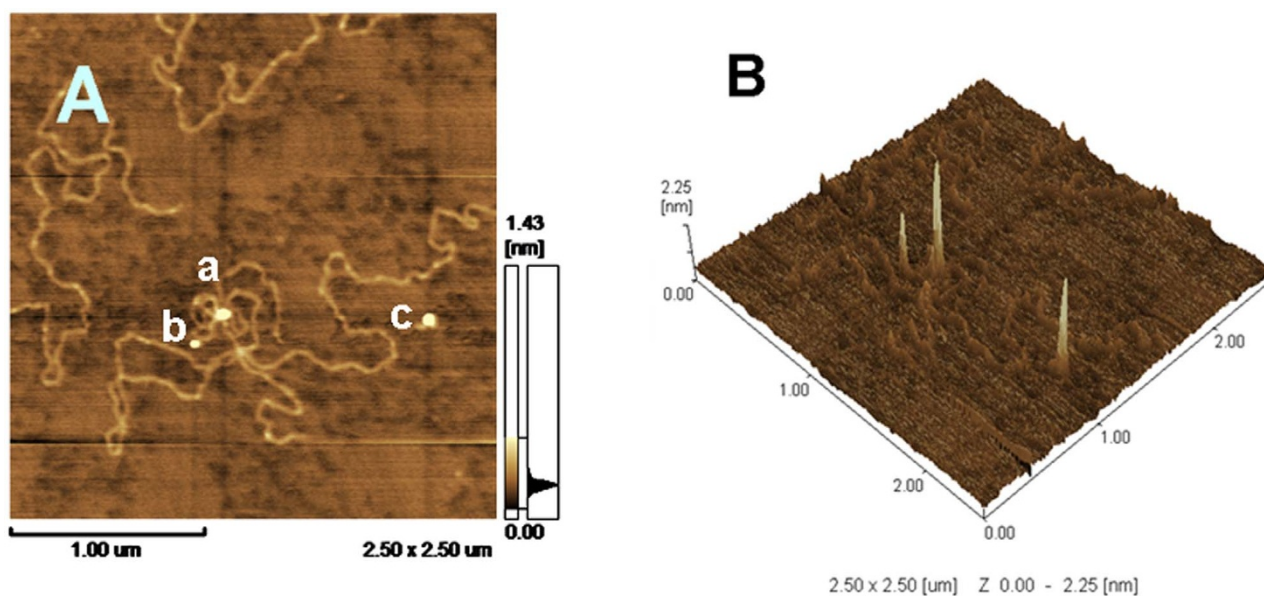

Figure 3 | AFM images of pure protein and protein-DNA complex, under enzyme concentration of 2.5 units/mL. A. The images of BspMI-DNA complex, with the DNA loop formation induced by an enzyme tetramer or enzyme aggregate. The number of loops around the protein (a) is greater than one. B. The three-dimensional height photograph of BspMI-DNA constructs on mica surface. The height of BspMI-DNA complex (a) is higher than the height of one tetramer (b).
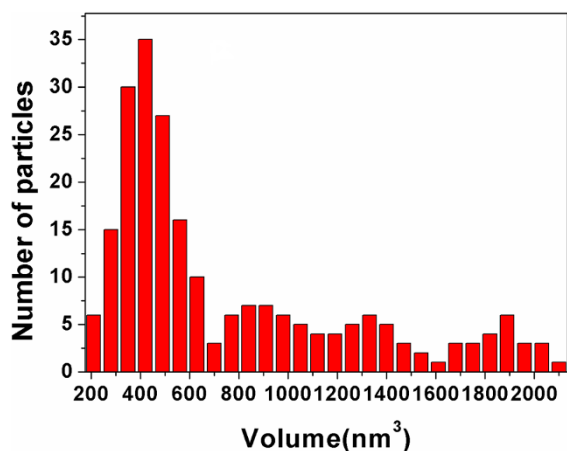
Figure 4 | Volume distribution of protein particles after 30 min incubation time, which revived the constructs of the enzymes. The sample size of protein particles is about 250 proteins from 25 different samples. The measured volumes of BspMI-DNA comprise three statistical peaks around 900 nm³, 1350 nm³, and 1900 nm³. These peaks correspond to the aggregations of 2, 3 and 4 BspMI particles, respectively. The proteins are single tetramers most of the time, but occasionally several tetramers combine to form an aggregate. From the volume distribution of the BspMI protein at less than saturation concentration, we found that the number of single tetramer BspMI -DNA particle constitutes over 85% of observed complexes.

form under certain conditions, such as long incubation time or high protein concentrations.

We used Pbr322 DNA, which has only one binding site to BspMI, as a control to examine non-specific binding of BspMI to DNA and the extent of protein-protein aggregation. From the AFM image shown in figure S1 we conclude that there is indeed non-specific binding and protein-protein aggregation. Details are elaborated in the supplementary information.

Volume and morphologies of BspMI-DNA complex in AFM images. AFM can be useful in the physical study of DNA-protein interactions. Loop formation in DNA can be induced by one BspMI tetramer binding two sites of DNA. From volume measurements of protein particles shown in Figure 3A we conclude that the enzyme complexes mostly comprise a single tetramer (b), although aggregates of more tetramers can also occur (c) and the number of loops around the protein is greater than one (a). Figure 3B shows the heights of the enzymes bound or unbound to DNA. The height of BspMI-DNA complex (a) is greater than the height of a single tetramer (b). So we supposed that proteins (a) and (c) are the aggregates of several tetramers.

AFM images show bound protein particles such as (a) in Figure 3A attached along the lambda-DNA. The loop can be clearly seen along the BspMI-DNA complex. This particle had a diameter at half-height of 47.0 nm and a height of 2.1 nm, giving an estimated single molecule volume of 1830 nm³. This volume is roughly equal to the four-fold volume one tetramer and reveals that DNA loops induced by BspMI can form by enzyme aggregates. Figure 4 shows the distribution of protein particle volumes obtained from 25 samples amounting to a total of 250 particles. The measured volume of BspMI-DNA complex ranges from less than 800 nm³ to greater than 2000 nm³, with three statistical peaks around 900 nm³, 1350 nm³ and 1900 nm³. These peaks correspond to aggregates of 2, 3 and 4 BspMI particles, respectively. Thus, the proteins are tetramers most of the time, can also be found in the form of aggregates composed of two or more tetramers. After an incubation time of 30 minutes and at enzyme concentrations less than saturation concentration, the BspMI single molecule volume distributions establish that single tetramer BspMI-DNA complexes comprise over 85% of observed particles.

Calibrating the size and volume of BspMI is a key to analyzing the aggregation of the proteins. Therefore we used avidin, a protein of known size, as a control. In the control measurement, we used a tetramer of avidin in order to calibrate the data in Figure 5. Dimensions of the avidin tetramer were measured to be 25 ±
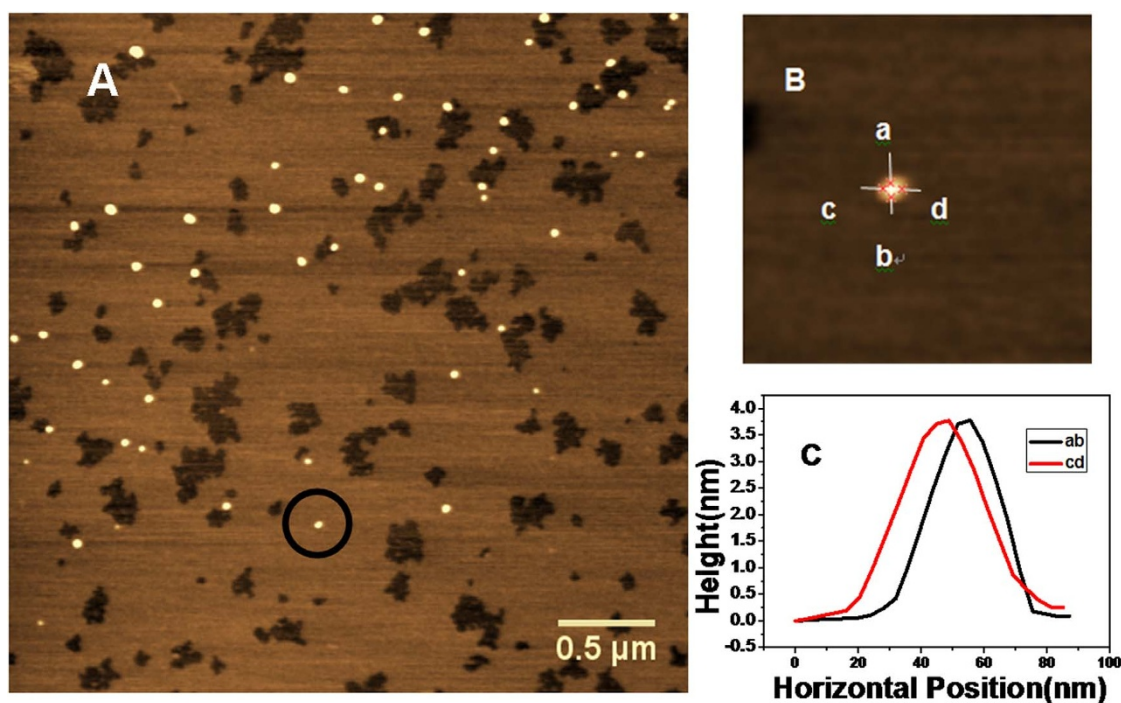

Figure 5 | The AFM images of avidins. The image shown in panel B is an enlarged part of the circle shown in panel A. Panel C shows the dimensions of avidin measued by with the software SPM9600 along the directions of a–b and c–d. The lengths of the major and minor axis were calculated using full width at half maximum.
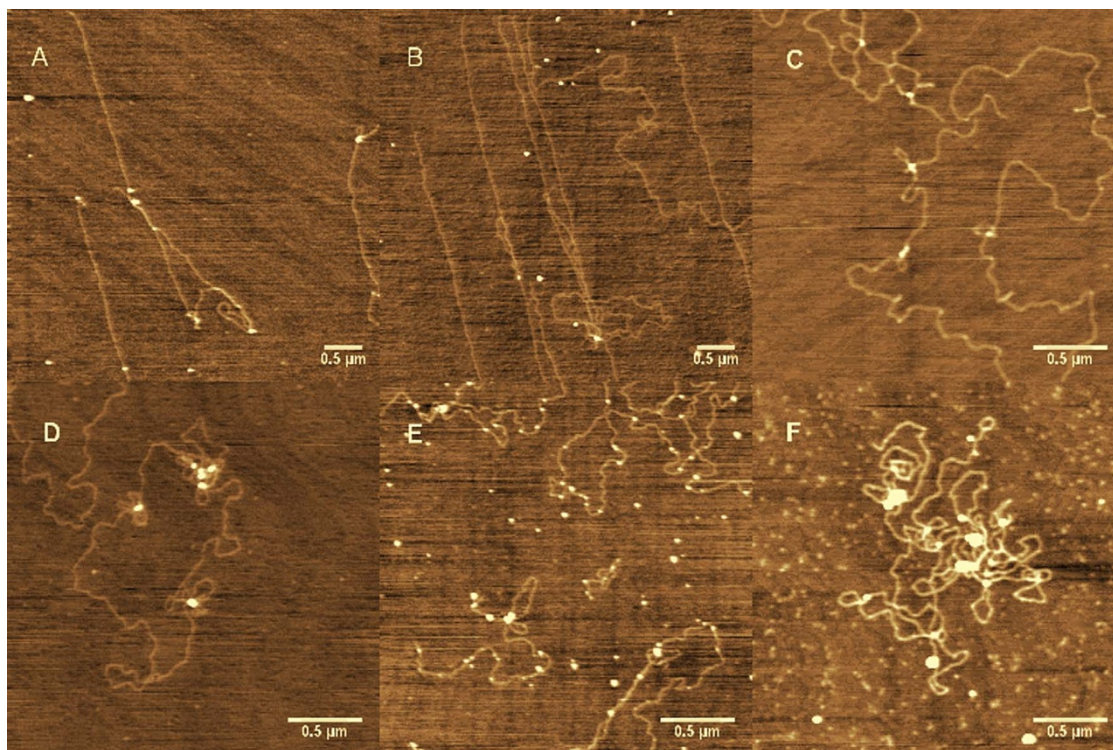
Figure 6 | AFM images of BspMI-DNA complexes. Panels A to F show BspMI binding the specific DNA sites and joining two specific DNA sites to form loops. The concentrations of the BspMI used in panels A to F were 1.25 units/mL, 2.5 unist/mL, 3.75 units/mL l, 5 units/mL l, 6.25 units/mL l, and 7.5 units/mL, respectively. All scale bars are 0.5 μm. AFM images of DNA-BspMI complexes show that binding and looping events increase with enzyme concentration.

4 nm (major axis, N = 30) and 17 ± 3 nm (minor axis, N = 30) by using the software of SPM9600 (Figure 5B and 5C). The major axis and minor axis lengths were analyzed using full width at half maximum shown Figure 5C. These results are consistent with existing values[34]. Under same deposition conditions and with the same tip, we measured different DNA molecules and found that their sizes agree to high accuracy with values reported in Ref. 32. In our measurement of BspMI, we applied the same deposition and tip as for avidin to make ensure reliability of the volume measurements. As for protein aggregation, the relative comparison is more important. Thus, we have compared relative sizes of protein complexes within one scan set to distinguish the single BspMI enzyme and their multiple aggregations.

The number of bound proteins and loops increased with the concentration of BspMI. From the AFM images, we find that the proteins not only bind one site of DNA, but also bind two sites to form loops. In Figure 6, the BspMI-DNA complex induced by different enzyme concentrations is shown on a mica surface. We use six concentrations of BspMI: 1.25 units/mL, 2.5 units/mL, 3.75 units/mL, 5 units/mL, 6.25 units/mL, and 7.5 units/mL. AFM images of DNA-BspMI complex shown in Figure 6A-D reveal that under conditions where the enzyme concentration is less than the critical concentration of 6 units/mL, binding and looping increases with increasing enzyme concentration. Figure 7 shows measurements of the single-molecule volume of the BspMI-DNA complex along with the distribution of single site binding and looping at concentrations below saturation concentration. We find that after a 30 minute incubation time, the number of single tetramer BspMI - DNA particles occupy over 85% of the bound enzymes. At the critical concentration of 6 units/mL in Figure 6E, all the BspMI binding sites are saturated, so the loops induced by one tetramer BspMI binding to two sites do not occur. However, when the concentration of the proteins is increased to 7.5 units/mL and the incubation time of

DNA and protein mixture is longer than 2 hours, protein-protein interactions become significant. The resulting additional loops induced by protein-protein interaction are shown in Figure 6F.

Statistics of DNA loops sites induced by BspMI. According to the binding sequence of lambda-DNA,loop sizes ranging from 9 bp to 47860 bp are theoretically possible. Our analysis of loop size
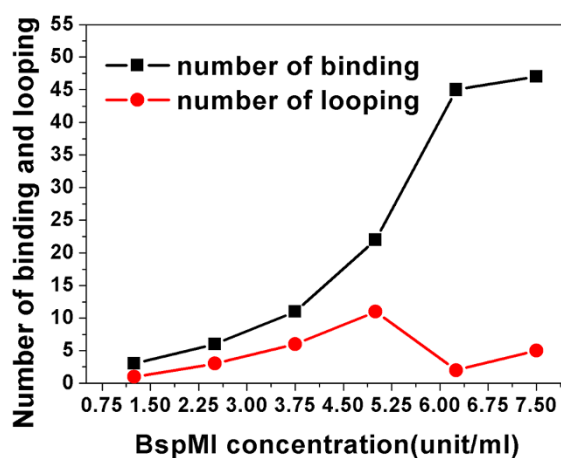

Figure 7 | Distribution of binding and looping events. The concentrations of BspMI employed were 1.25 units/mL, 2.5 units/mL, 3.75 units/mL, 5 units/mL, 6.25 units/mL, and 7.5 units/mL. At the critical concentration of 6 units/mL, all the BspMI binding sites were saturated. As a result, the loop formation by a single BspMI tetramer binding to two binding sites was inhibited. However, when the protein concentration was increased to 7.5 units/mL and the incubation time of DNA and protein mixture was longer than 2 hours, protein-protein interactions could occur.
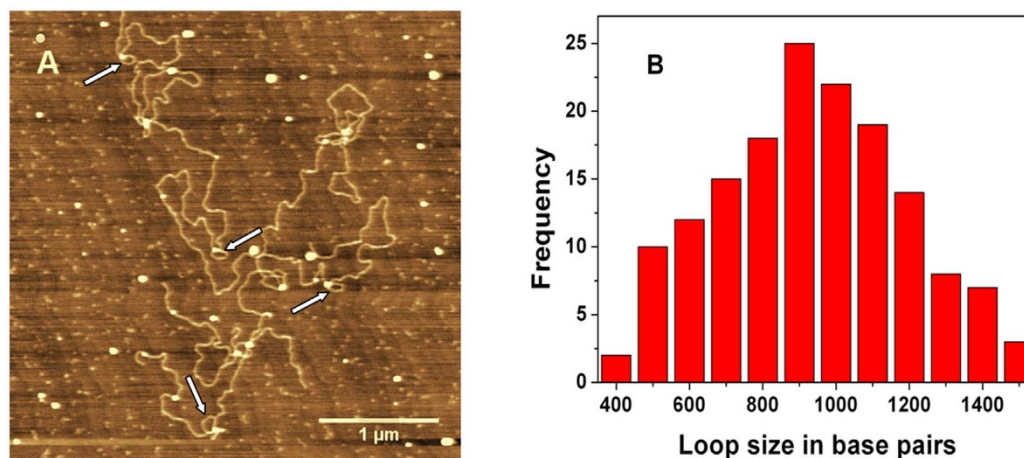
Figure 8 | AFM images of BspMI-DNA looped constructs and distribution of loop sites on the 39 specific binding sites of lambda-DNA.
Panel A shows a single BspMI binding DNA on specific two sites and them to form a loop. Four loops are clearly visible on the DNA thread (see arrows).
Panel B shows the loop site distribution for looped BspMI-DNA constructs. The distribution of measured loop sizes was peaked at about 900 bp.

distribution of loops induced by protein binding revealed a strong peak around 900 bp, as shown in in Figure 8. However, the width of the distribution allows for a wide range of loop sizes ranging from 400 bp to 1500 bp. This suggests that the specific binding sites on DNA are asymmetrically distributed and that the second loop structures are not caused by a single protein molecule binding to two sites. We suppose that this structure was induced by protein-protein interaction.

Evidence for DNA-BspMI complex through MT. We used a 3D translation stage (MP-285) to move a magnetic bead allowing the 16 μm DNA molecule to encounter itself in a solution of different concentrations of BspMI in PBS and 100 μM CaCl$_2$. After incubation for 5 min, we released the magnetic bead, thus placing the molecule under tension of 1 pN applied by the magnet for 10 min (Figure 9A) or 2 hours (Figure 9B). For the data shown in Figure 9A, the protein concentration was kept low and the incubation time of the complex was 10 minutes. In contrast, the data shown in Figure 9B was taken under protein concentrations greater than saturation concentration and the incubation time of the complex was 2 hours. We then exerted greater force on the magnet to look at the extension change of DNA. A series of jumps in DNA extension was

observed, the size ranged from roughly 100 nanometers to a few microns, as the loops were opened. In Figure 9A the jumps are about 120 nm, 100 nm, 180 nm, at a force of about 3.64 pN (refer to time interval from 1320 s to 1400 s). The upper inset in Figure 9A shows the distribution of pulling force on the loops under low BspMI concentration. The force is peaked at 3 pN. In Figure 9B, if the BspMI is higher than the saturation concentration, we cannot observe the loops at short times. However, a series of jumps would occur after the incubation is longer than three hours at a force of 6.2 pN. In the single-molecule pulling experiment, the displacements of the microsphere are in the range of micrometers, corresponding to a change in applied magnetic force less than 0.03 pN. In most cases, errors of the measurement are less than 5%. Therefore, the force can be considered as constant, and needs no further adjustment in the experimental process.

When the concentration of BspMI is lower than the saturation concentration jumps occur at a broad distribution of forces, as shown in Figure 9A. In Figure 9B, due to the large protein concentration, the specific binding sites on DNA are saturated and loop formation is inhibited. Thus, we hardly see any jumps in the MT experiment. But if we increased the incubation time beyond three hours, the loops could again be formed, induced by protein-protein interaction.
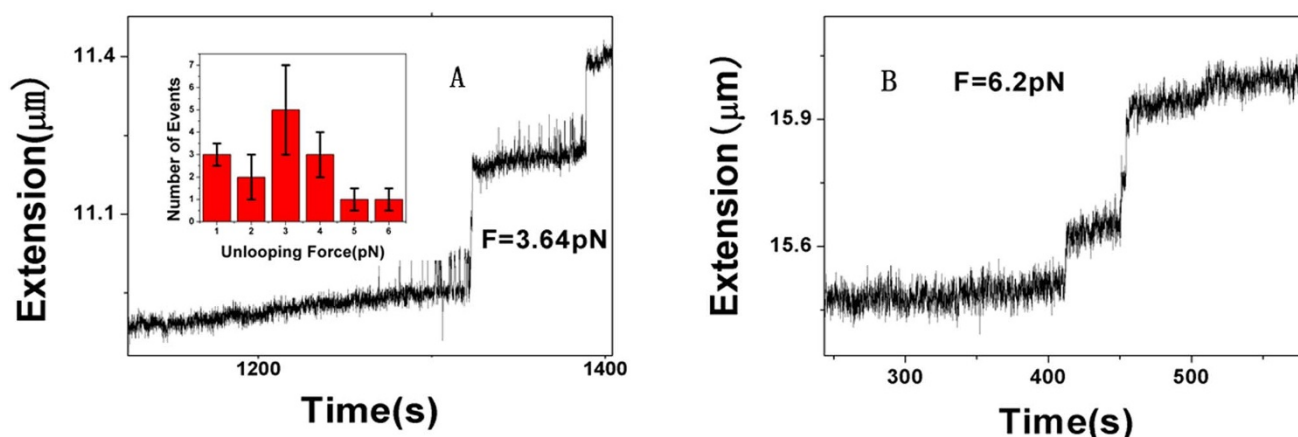

Figure 9 | Time series, at different forces, for opening of loops along λ-DNA formed by BspMI. Panel A shows results with BspMI concentration of 2.5 units/mL and the complex incubated for 10 min. The upper inset shows the pulling force distribution pulling under lower soncentration of BspMI. The was peaked at 3 pN. Panel B shows results with BspMI concentration of 6.25 units/mL and the complex incubated for more than 2 hours. With BspMI higher than the saturation concentration, loops could not be observed at short times. However, a series of jumps would occur at a force of 6.2 pN when the incubation was longer than three hours.
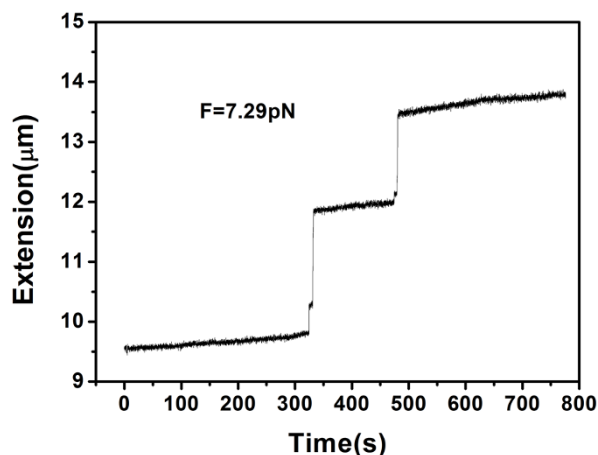
Figure 10 | Un-looping force at 5 mM CaCL₂ concentration. The rupture force increased to about 7 pN with the BspMI concentration of 3 units/mL.

Jumps occur in the extension time series. We supposed that there are two ways in which BspMI can induce DNA loop formation, as depicted in Figure 11. One is that one BspMI tetramer bind the two sites, and the other is that the is loop formed by an aggregate of BspMI tetramers.

There seems to be a major discrepancy between the rupture forces in this paper and previous work by Smithet al[4]. However, we used a different buffer and our $CaCl_2$ concentration was much lower than in the abovementioned literature. The enzyme buffer of BspMI used by themwas 50 mM tris-HCl, 100 mM NaCl, 10 mM $CaCl_2$, and 1 mM DTT. The enzyme buffer we used was PBS containing 0.1 mM $CaCl_2$. We measured loop disruption forces for a single BspMI tetramer around 3 pN at 0.1 mM $CaCl_2$ concentration, which are consistent with the critical rupture forces under same conditions as reported by

(Ref 3). In fact, they already pointed out the strong dependence of the rupture force on the concentration of calcium ions by measuring up to twofold increase in rupture force with increasing calcium concentration[4]. We did additional control experiments at 5 mM $CaCl_2$ concentration but with the same buffer conditions. The result is shown in Figure 10. The rupture force is indeed increased to about 7 pN. In fact, at 0.1 mM calcium concentration, our rupture force is still in the same order with those reported by Smith group.

The model of BspMI-DNA complex. The capture of a DNA loop of fixed length by the concurrent binding of BspMI to two separate sites in the DNA can be accounted for by least two different schemes. In the first, the protein exists in a tetramer state that enables it to bind directly to both DNA sequences[35], i.e., the native protein possesses two separate surfaces for binding DNA (Figure 11A). In the second, the protein exist an aggregate state that binds two or more sites (Figure 11B).

The aspects of DNA structure (supercoiling, site separation, and so forth) influenced loop stability by binding a single tetramer protein (Figure 11A). Looping by binding a single tetramer protein with two DNA-binding surfaces is inevitably blocked at high concentrations of the protein[36] because the DNA must then bind a separate molecule of the protein at each target site (Figure 11A). The disruption of the loop by an excess of one binding tetramer protein may be of little consequence for an enzyme reaction. The disruption by excess protein may, however, have severe consequences for a regulatory system, for example, where the level of gene expression is determined by the equilibrium distribution between looped and un-looped states[35]. In our experiments, the incubation time is long enough that the DNA-BspMI loops can form owing to the aggregates among proteins (Figure 11B). From the AFM images in Figure 11, we can see that the BspMI-DNA complex can have many kinds of constructs, such as one loop-enzyme complex, two loop-enzyme complex, three loop-enzyme complex, and four loops-enzyme complex.
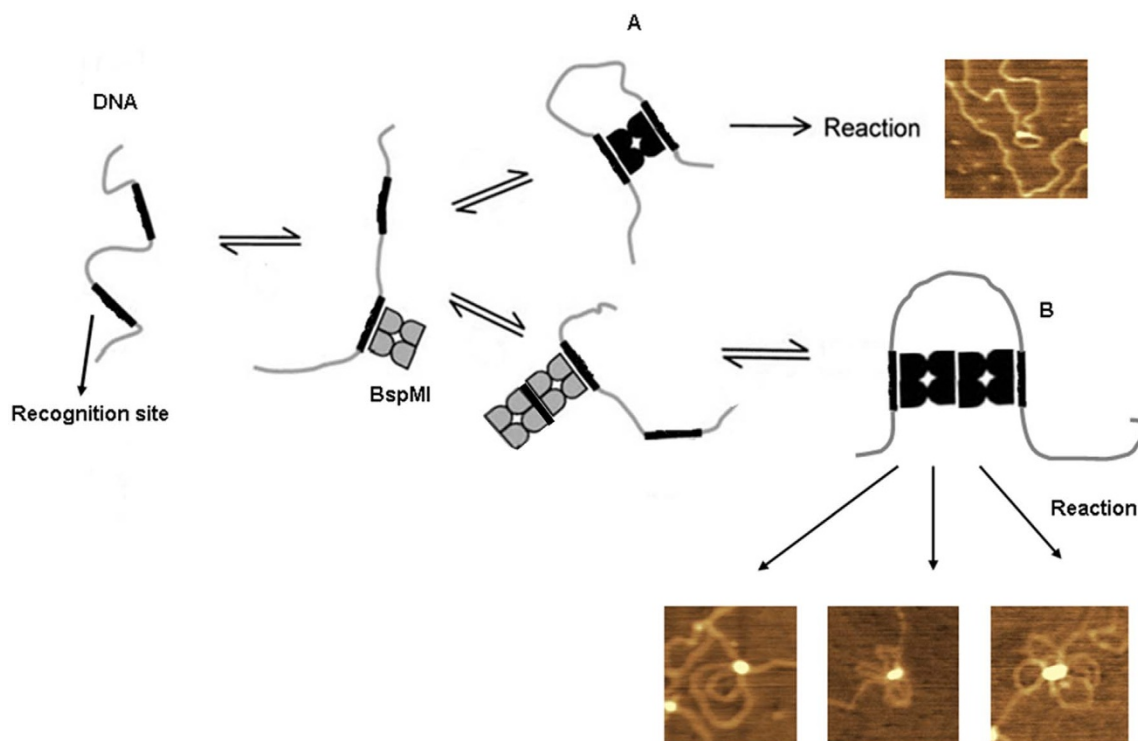

Figure 11 | Loop capture by (A) preassembled protein on DNA. The tetrameric protein (four gray subunits) binds first to one copy of its palindromic recognition sequence (head-to-head arrows) via two protein subunits (the flat edges mark the DNA-binding surface), and then to the second copy via its other subunits: This causes a conformational change in all four subunits (denoted in black). (B) The DNA with a tetramer bound at one site form loops by binding a second tetramer at the other site.

Conclusions

In summary, the specific and nonspecific binding of enzyme to DNA was observed in AFM images and confirmed in single molecular pulling by magnetic tweezers. At saturating enzyme concentrations, when the 39 specific binding sites have been occupied for lambda DNA, more than 8% total BspMI-DNA complexes are due to non-specific binding. In this case, there are few DNA loops induced by a single enzyme binding to two sites. Below the saturation concentration, the numbers of both one site binding and two site looping increase with the BspMI concentration. Meanwhile, we observed additional loops by enzyme aggregation when the BspMI concentration is at or above saturation concentration and for long incubation times. The DNA-BspMI complex pulling experiment of magnetic tweezers shows that the enzyme aggregation is stronger (>6 pN) than its binding to DNA (about 3 pN). Therefore, enzyme aggregation might play an important role in the interaction between DNA and two site binding restriction endonuclease proteins.

1. van Gent, D., Hoeijmakers, J. & Kanaar, R. Chromosomal stability and the DNA double-stranded break connection. *Nature Reviews Genetics* **2**, 196–206 (2001).
2. Shin, D., Chahwan, C., Huffman, J. & Tainer, J. Structure and function of the double-strand break repair machinery. *DNA repair* **3**, 863–873 (2004).
3. Yan, J., Skoko, D. & Marko, J. Near-field-magnetic-tweezer manipulation of single DNA molecules. *Physical Review E* **70**, 11905–11909 (2004).
4. Gemmen, G. J., Millin, R. & Smith, D. E. DNA looping by two-site restriction endonucleases: heterogeneous probability distributions for loop size and unbinding force. *Nucleic acids research* **34**, 2864–2877 (2006).
5. Mücke, M. et al. Imaging DNA Loops Induced by Restriction EndonucleaseEcoRII. *Journal of Biological Chemistry* **275**, 30631–30637 (2000).
6. Topal, M., Thresher, R., Conrad, M. & Griffith, J. NaeI endonuclease binding to pBR322 DNA induces looping. *Biochemistry* **30**, 2006–2010 (1991).
7. Siksnys, V. et al. The Cfr10I restriction enzyme is functional as a tetramer1. *Journal of molecular biology* **291**, 1105–1118 (1999).
8. Friedhoff, P., Lurz, R., Lüder, G. & Pingoud, A. Sau3AI, a monomeric type II restriction endonuclease that dimerizes on the DNA and thereby induces DNA loops. *Journal of Biological Chemistry* **276**, 23581–23586 (2001).
9. Berge, T., Ellis, D. J., Dryden, D. T., Edwardson, J. M. & Henderson, R. M. Translocation-Independent Dimerization of the Eco KI Endonuclease Visualized by Atomic Force Microscopy. *Biophysical journal* **79**, 479–484 (2000).
10. Neaves, K. J. et al. Atomic force microscopy of the EcoKI Type I DNA restriction enzyme bound to DNA shows enzyme dimerization and DNA looping. *Nucleic acids research* **37**, 2053–2063 (2009).
11. Pastre, D. et al. Specific DNA- Protein Interactions on Mica Investigated by Atomic Force Microscopy. *Langmuir* **26**, 2618–2623 (2009).
12. Harada, Y. et al. Direct observation of DNA rotation during transcription by Escherichia coli RNA polymerase. *Nature* **409**, 113–115 (2001).
13. Lushnikov, A., Potaman, V., Oussatcheva, E., Sinden, R. & Lyubchenko, Y. DNA Strand Arrangement within the SfiI- DNA Complex: Atomic Force Microscopy Analysis. *Biochemistry* **45**, 152–158 (2006).
14. Reich, S., Gossl, I., Reuter, M., Rabe, J. P. & Krüger, D. H. Scanning force microscopy of DNA translocation by the Type III restriction enzyme EcoP15I. *Journal of molecular biology* **341**, 337–344 (2004).
15. Lushnikov, A. Y., Potaman, V. N. & Lyubchenko, Y. L. Site-specific labeling of supercoiled DNA. *Nucleic acids research* **34**, e111–e111 (2006).
16. Crampton, N. et al. Fast-scan atomic force microscopy reveals that the type III restriction enzyme EcoP15I is capable of DNA translocation and looping. *Proceedings of the National Academy of Sciences* **104**, 12755–12760 (2007).
17. Sorel, I. et al. The EcoRI-DNA complex as a model for investigating protein-DNA interactions by atomic force microscopy. *Biochemistry* **45**, 14675–14682 (2006).
18. Halford, S., Welsh, A. & Szczelkun, M. Enzyme-mediated DNA looping. *Annual Review of Biophysics and Biomolecular Structure* **33**, 1–24 (2004).
19. Deibert, M., Grazulis, S., Sasnauskas, G., Siksnys, V. & Huber, R. Structure of the tetrameric restriction endonuclease NgoMIV in complex with cleaved DNA. *Nature Structural & Molecular Biology* **7**, 792–799 (2000).
20. Bilcock, D., Daniels, L., Bath, A. & Halford, S. Reactions of type II restriction endonucleases with 8-base pair recognition sites. *Journal of Biological Chemistry* **274**, 36379–36386 (1999).
21. Wentzell, L., Nobbs, T. & Halford, S. TheSfiI Restriction Endonuclease Makes a Four-strand DNA Break at Two Copies of its Recognition Sequence. *Journal of molecular biology* **248**, 581–595 (1995).
22. Embleton, M., Siksnys, V. & Halford, S. DNA cleavage reactions by type II restriction enzymes that require two copies of their recognition sites1. *Journal of molecular biology* **311**, 503–514 (2001).
23. Gormley, N., Hillberg, A. & Halford, S. The type IIs restriction endonuclease BspMI is a tetramer that acts concertedly at two copies of an asymmetric DNA sequence. *Journal of Biological Chemistry* **277**, 4034–4041 (2002).
24. Bath, A., Milsom, S., Gormley, N. & Halford, S. Many type IIs restriction endonucleases interact with two recognition sites before cleaving DNA. *Journal of Biological Chemistry* **277**, 4024–4033 (2002).
25. van Noort, S. J. T. et al. Direct visualization of dynamic protein-DNA interactions with a dedicated atomic force microscope. *Biophysical journal* **74**, 2840–2849 (1998).
26. Lyubchenko, Y. L. & Shlyakhtenko, L. S. AFM for analysis of structure and dynamics of DNA and protein-DNA complexes. *Methods* **47**, 206–213 (2009).
27. Schneider, S., Lürmer, J., Henderson, R. & Oberleithner, H. Molecular weights of individual proteins correlate with molecular volumes measured by atomic force microscopy. *Pflügers Archiv European Journal of Physiology* **435**, 362–367 (1998).
28. Sun, B. et al. Impediment of E. coli UvrD by DNA-destabilizing force reveals a strained-inchworm mechanism of DNA unwinding. *The EMBO Journal* **27**, 3279–3287 (2008).
29. Strick, T., Allemand, J., Bensimon, D. & Croquette, V. Behavior of supercoiled DNA. *Biophysical journal* **74**, 2016–2028 (1998).
30. Smith, S., Finzi, L. & Bustamante, C. Direct mechanical measurements of the elasticity of single DNA molecules by using magnetic beads. *Science* **258**, 1122–1126 (1992).
31. Vanamee, S., Santagata, S. & Aggarwal, A. FokI requires two specific DNA sites for cleavage1. *Journal of molecular biology* **309**, 69–78 (2001).
32. Wyman, C., Rombel, I., North, A. K., Bustamante, C. & Kustu, S. Unusual oligomerization required for activity of NtrC, a bacterial enhancer-binding protein. *Science* **275**, 1658–1661 (1997).
33. Lyubchenko, Y. L. Preparation of DNA and nucleoprotein samples for AFM imaging. *Micron* **42**, 196–206 (2011).
34. Sun, H. B., Qian, L. & Yokota, H. Detection of abasic sites on individual DNA molecules using atomic force microscopy. *Analytical chemistry* **73**, 2229–2232 (2001).
35. Schleif, R. DNA looping. *Annual review of biochemistry* **61**, 199–223 (1992).
36. Szczelkun, M. & Halford, S. Recombination by resolvase to analyse DNA communications by the SfiI restriction endonuclease. *The EMBO Journal* **15**, 1460–1469 (1996).

Author contributions

G.C.Y. conceived the work. Y.W.W. performed the experiments. S.Y.R. assisted with the experiments and data analysis. G.C.Y. and Y.W.W. analyzed the data and prepared the manuscript.

Additional information